

ON ABSORPTION SPECTRA OF $\text{CoCl}_2/\text{ACETONE}$ SYSTEMS

G. Stanescu, Ath. Trutia *

Bucharest University, Faculty of Physics, POB MG-11, Bucharest, Magurele 077125, Romania

The absorption spectra of $\text{CoCl}_2/\text{acetone}$ systems were measured and analysed. Adding LiCl to the $\text{CoCl}_2/\text{acetone}$ solutions forced a stepwise formation of higher, negatively charged, chloro-Co-systems. The second derivative method was used to reveal the elemental absorption band positions of these tetrahedral and tetrahedral-like Co-complexes. A computer simulated experiment was performed to study the method's limitations. A doubt is raised concerning the accuracy of some literature data.

(Received March 9, 2005; accepted March 23, 2005)

Keywords: UV-VIS spectroscopy, Tetrahedral Co-complexes, Band peak detection

1. Introduction

The study of the cobalt halides in organic solvent has been pioneered by Katzin [1] several decades ago. During the 50s, he was one of the first researchers who used optical spectroscopic data to analyze cobalt salts structures. One decade later, Fine [2] and Trutia [3], among others, revealed the presence of several types of complexes in some of these systems. Those studies offered the grounds for better understanding spectral data, and for the development of the crystal field theory.

In this paper we return to the spectroscopic studies of cobalt complexes in acetone solution, which have been initially studied by Fine [2], since they show similarities with cobalt halides in PEG (PolyEthylene Glycol), which have been studied lately [4 – 6]. Fine studied the spectra of CoCl_2 , CoBr_2 and CoI_2 in acetone solutions and he identified the types of complexes which exist in these solutions and analysed their spectra.

2. Experimental

We have used a Varian, dual beam, Cary Model 118 spectrophotometer, to study the visible (500-800 nm) spectrum of CoCl_2 in acetone solutions. The scanning speed was 2 nm/s, with 1 nm recording steps. The data have been acquired using a PC with a CMA UIB 12 bit interface and a custom software package. All the experiments have been performed at room temperature (20 °C). The Cobalt Chloride was dried in a vacuum oven at 120 °C for 3 hours. Then, the dried Cobalt Chloride has been dissolved in acetone, and the absorption spectrum recorded (Fig. 1, curve 1) using a 2 mm path-length glass cell.

This solution has a tetrahedral-type Co-complexes with two chlorines and two acetones. The fact that they are tetrahedral-like is obvious since their spectra are in the right place and very intense. This last feature is a consequence of the absence of inversion centre for tetrahedral complexes; the electric-dipole transitions are thus allowed according to the Laporte's rule. So, the spectrum of this $\text{CoCl}_2/\text{acetone}$ solution is assigned to the $[\text{CoCl}_2\text{Ac}_2]$ -complex. When LiCl is added to the initial solution, thus supplying more Cl^- ions, the spectrum changes, to other species of the Co-complexes. If the LiCl is added in small steps, the spectra of these new species can be detected. For this purpose, a small amount of LiCl has been combined with some of the initial solution, and this has been added to the original solution in small amounts. Some of these absorption spectra are shown in Fig. 1 and 2.

* Corresponding author: trutia@infim.ro

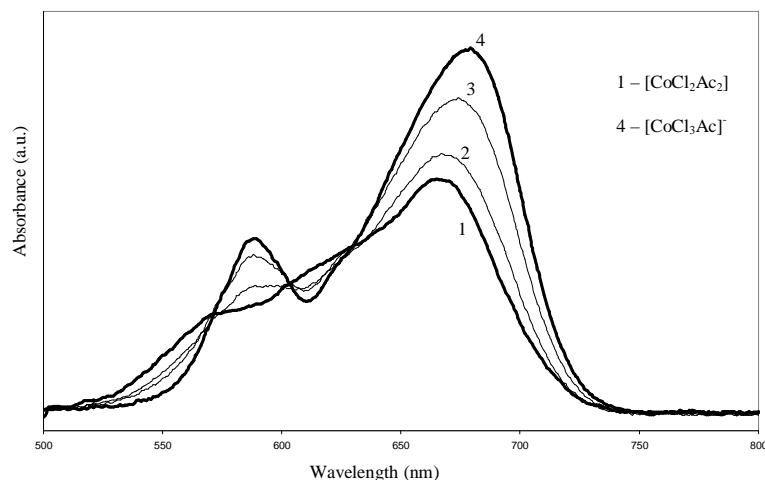


Fig. 1. Changes of the CoCl_2 /acetone absorption spectrum when LiCl is stepwisely added.

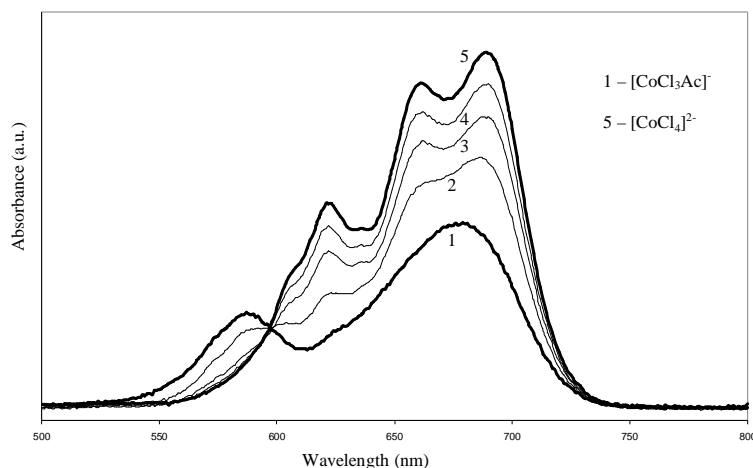


Fig. 2. Further modification of CoCl_2 /acetone spectrum following LiCl addition until the $[\text{CoCl}_4]^{2-}$ complex is formed.

3. Results and discussion

There are three types of complexes depending on the added LiCl concentration of (actually on the concentration of Cl^- ions added to the solution). These three types of complexes are $[\text{CoCl}_2\text{Ac}_2]$, $[\text{CoCl}_3\text{Ac}]^-$ and $[\text{CoCl}_4]^{2-}$ where Ac is a ligand from the acetone molecule (probable the Oxygen atom). Fig. 1 shows the change from the $[\text{CoCl}_2\text{Ac}_2]$ -complex spectrum (spectrum 1, initial sample, without LiCl) to the spectrum of the $[\text{CoCl}_3\text{Ac}]^-$ -complex (spectrum 4), identified by the peak at 590nm, corresponding to this type of Co-complexes. Here we must make a few commentaries. Literature data [2] shows, that in the transformation process, the $[\text{CoCl}_3\text{Ac}]^-$ -complexes appear first, and only when this process ends, when all the Co-complexes are of this type, the $[\text{CoCl}_4]^{2-}$ -complex starts building up. The existence of three isobestic points in Fig. 1 shows that there are only two absorbent species in these samples, which convert from one to another when the Cl^- ion concentration increases (the ratio of Cl/Co increases from 2 to 3).

The transition from the $[\text{CoCl}_3\text{Ac}]^-$ spectrum to that of the $[\text{CoCl}_4]^{2-}$ is shown in Fig.2. According to the literature data [3, 2], the development of the $[\text{CoCl}_4]^{2-}$ complex does not stop once the Cl/Co ratio reaches 4, but continues even beyond 8, because this complex is more unstable due to a higher dissociation degree. The presence of the isobestic points, in both sequences of transformation (Fig. 1 and 2), proves the presence of two species only, in each of the two cases.

These spectra can be associated with real tetrahedral (T_d), or pseudo-tetrahedral complexes (most probably C_{3v} and C_{2v}). For the case of $[CoCl_2Ac_2]$ and $[CoCl_3Ac]^-$, the acetone ligand occupies an apex of the tetrahedron and therefore the complex remains mainly tetrahedral.

Table 1. The band positions of the $[CoCl_2Ac_2]$, $[CoCl_3Ac]^-$ and $[CoCl_4]^{2-}$ -complexes.

Complex	Peak	Our results		Fine [2]	
		$\tilde{\nu}$ (cm ⁻¹)	λ (nm)	$\tilde{\nu}$ (cm ⁻¹)	λ (nm)
$[CoCl_2Ac_2]$	1	14900	671	14800	674
	2	16025	624	15900	~630(sh)
	3	17575	569	17400	575
$[CoCl_3Ac]^-$	1	14575	686	14500	688
	2	16050	623	15900	~630(sh)
	3	17025	587	17000	590
$[CoCl_4]^{2-}$	1	14425	693	14400	697
	2	15200	658	15000	667
	3	15750	635	15600	~640(sh)
	4	16100	621	16000	625
	5	16550	604	16400	~610(sh)

According to the crystal field theory, the main absorption in the visible spectrum for a tetrahedral cobalt complex is associated with the $^4A_2(F) \rightarrow ^4T_1(P)$ transition. For the $[CoCl_3Ac]^-$ and $[CoCl_2Ac_2]$ -complexes, the lowering symmetries from T_d to C_{3v} and, C_{2v} respectively, should produce the splitting of this band, which is confirmed by the spectra seen in Fig 1 and 2. The presence of several bands for the $[CoCl_4]^{2-}$ is still not well understood. If we were to explain these bands as an effect of the lowering symmetry this becomes even more intriguing since its spectrum shows even more elemental bands than the spectra of the $[CoCl_2Ac_2]$ and $[CoCl_3Ac]^-$ -complexes. We could consider the descending of the T_d symmetry due to the distortion of the tetrahedron, but this does not explain all the effects. Regardless of the symmetry, the ground state, 4A_2 , is a one-dimensional state, it does not split, and the excited, 4T_1 , state can split at most into three one-dimensional states (for the C_{2v} case). Therefore the symmetry alone cannot explain the presence of more than three bands. Literature [7] associates the apparition of two additional bands for the $[CoCl_4]^{2-}$ -complex to some spin forbidden transitions from the quartet 4A_2 ground state to the excited doublet states 2E and 2T_1 [8].

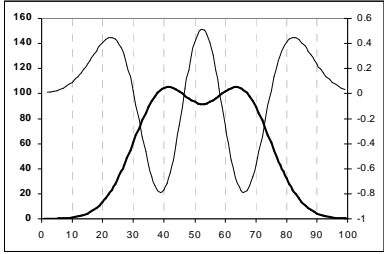
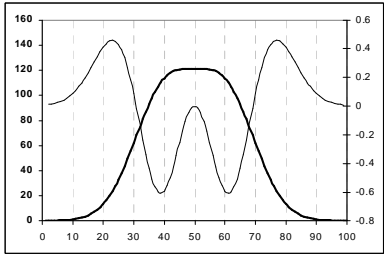
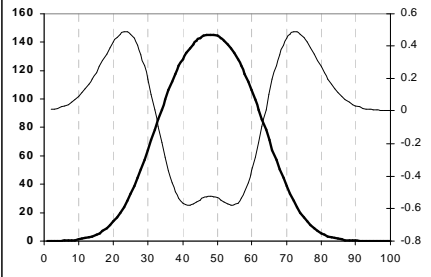
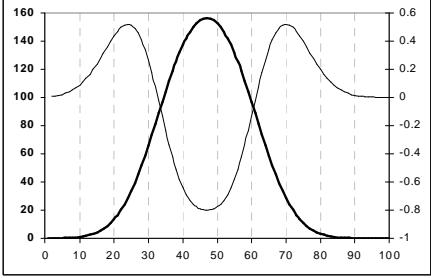
The position of the elemental spectral bands in Fig. 1 and 2 are shown in Table 1 and compared to the results of Fine [2]. In our case the second derivative method has been used to reveal the position of these bands. Usually the peaks of the local maxima in the input data will produce second derivative local minima with values that fall below zero. Small components of the spectrum, however, could be hidden (swallowed) by the near by bigger band-peaks and they do not show local maxima in the input spectrum. These peaks could eventually be found by the second derivatives, i.e. by the corresponding local minima with values that tend to be above or near zero. Therefore the method we are using to detect the hidden spectral bands is the second derivative minima.

In order to study this method, and to understand its limitations, we performed the following experiment. Working with computer simulated data, we mixed two Gaussian curves with different, varying, parameters:

$$y = a_0 e^{-\frac{1}{2} \left(\frac{x-a_1}{a_2} \right)^2} + b_0 e^{-\frac{1}{2} \left(\frac{x-b_1}{b_2} \right)^2} \quad (1)$$

where: a_0, b_0 – amplitude;
 a_1, b_1 – centre (peak);
 a_2, b_2 – width (standard deviation).

Table 2. The second derivative method (I).

Case	Position	Gauss 1	Gauss 2	Graph (sum - solid line, second derivative - thin line)
1	real	40	65	
	given by the second derivative	39	66	
	given by the local maximum	42	63	
2	real	40	60	
	given by the second derivative	39	61	
	given by the local maximum	50	50	
3	real	40	56	
	given by the second derivative	42	54	
	given by the local maximum	48	48	
4	real	40	54	
	given by the second derivative	47	47	
	given by the local maximum	47	47	

We calculated the second derivative of this „mathematical” spectrum, and then we studied the sensitivity of the method, for finding the initial band positions, as a function of the amplitude, spectral separation and width of the two Gaussians.

We started by mixing two Gaussians with the same amplitude ($a_0 = b_0 = 100$ a.u.) and the same width ($a_2 = b_2 = 10$ a.u.) but separated by various intervals on the wavelength scale (the x axis - in a.u.). The results and the graphs are shown in Table 2.

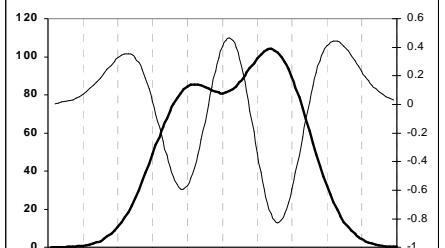
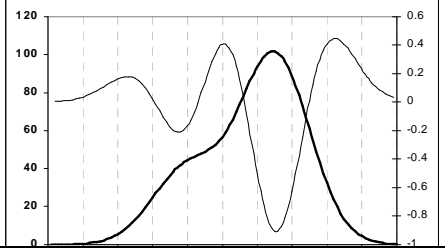
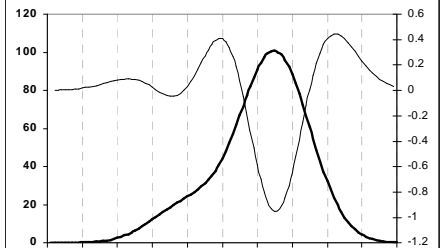
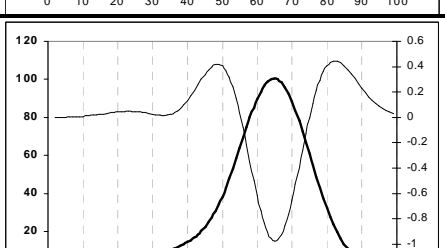
In the first case, the two curves were well separated so that each formed a local maximum; then the separation was decreased until we could not distinguish them anymore, not even using the second derivative method. In Table 2 we give the real position of the two Gaussians, the positions indicated by the second derivative method and the position of the local maxima (for the cases when local maxima occur). We should note the following observations:

- the second derivative method is able to resolve the two Gaussians even when they do not form local maxima (cases 2 and 3 – Table 2);
- the second derivative method's precision for determining the position of the Gaussian components is higher when they are well separated (case 1) compared to the direct local maxima method (the bands tend to approach one another);
- the peak's-position precision using the second derivative method decreases when the separation decreases (case 3), reaching an intrinsic method's limit as seen in case 4.

In Table 3 we mixed the same Gaussians, but we kept the positions ($a_1 = 40$ and $b_1 = 65$) and the widths ($a_2 = b_2 = 10$) fixed while varying the intensity of the first Gaussian (a_0) from 100 down to 10. The first Gaussian become, at the beginning of the process, a shoulder on the left hand side of the main band, before it disappear completely for an amplitude 10 times smaller than the main band. Here, again, we note a few things:

- the second derivative method can reveal the presence of the smaller (hidden) peak, but the precision decreases at very low intensities;
- the precision for the stronger peak position, although reasonable for case 5, improves when this peak becomes dominant (cases 6, 7, 8);

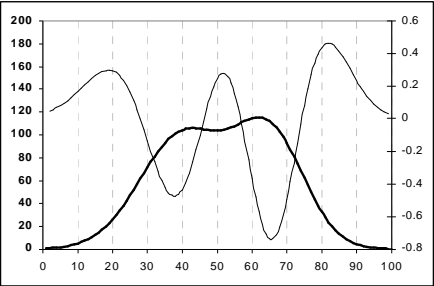
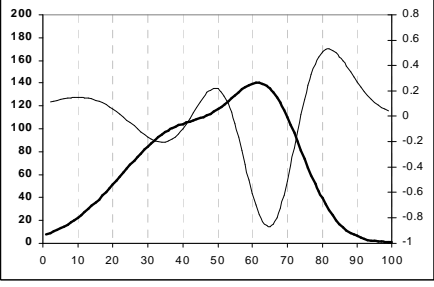
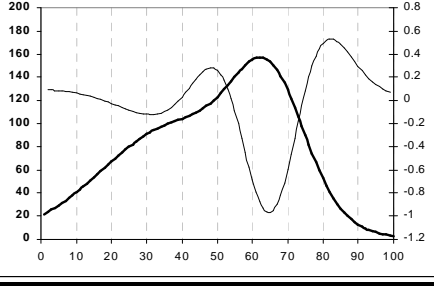
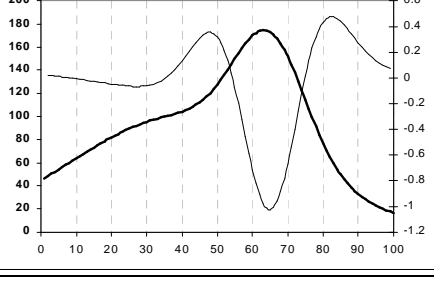
Table 3. The second derivative method (II).

Case		Gauss 1	Gauss 2	Graph (sum - solid line, second derivative - thin line)
5	Amplitude	80	100	
	Position: -real	40	65	
	- given by the second derivative	39	66	
6	Amplitude	40	100	
	Position: -real	40	65	
	- given by the second derivative	37	65	
7	Amplitude	20	100	
	Position: -real	40	65	
	- given by the second derivative	36	65	
8	Amplitude	10	100	
	Position: -real	40	65	
	- given by the second derivative	33	65	

In Table 4 we analyze the cases where the intensities ($a_0 = b_0 = 100$) and position ($a_1 = 40$ and $b_1 = 65$) are constant, but the width of the first Gaussian is varied from 12.25 to 31.62. The second Gaussian becomes dominant, while the first one becomes a shoulder and then disappears (but by getting wider, this time). The conclusions for this situation are:

- the second derivative method reveal the peaks in all cases, but the precision for the wide band becomes worse for Gaussians with large width (cases 11 and 12) and shifted towards outside compared to their real position;
- for the thinner peak the sensitivity to its position determination is great in any case and is improving when the peak become dominant (cases 10, 11 and 12).

Table 4. The second derivative method (III).

Case		Gauss 1	Gauss 2	Graph (sum - solid line, second derivative - thin line)
9	Width	12.25	10	
	Position: -real	40	65	
	- given by the second derivative	38	66	
10	Width	17.32	10	
	Position: -real	40	65	
	- given by the second derivative	34	65	
11	Width	22.36	10	
	Position: -real	40	65	
	- given by the second derivative	31	65	
12	Width	31.62	10	
	Position: -real	40	65	
	- given by the second derivative	27	65	

Returning now to our initial spectra (Fig. 1 and 2) we should mention that the analysis of real (measured) spectra is much more difficult compared to the simulated spectra. The simulated data are exact data (even perfect). Unlike that, the real data are affected by noise and imperfections,

therefore harder to be analyzed. The second derivative method fails sometimes because the noise could cause some of the calculated points to jump in the opposite direction, thus giving a false result. It is necessary for the spectrum to be processed first, i.e. to be smoothed. The smoothing is an operation of local averaging which remove noises from data (at least partially) and then the derivation becomes possible.

For these operations we used the PeakFit v.4 program, produced by Jandel Scientific, as a dedicated software for analyzing spectral data. With "Inspect 2nd Derivative" option of this software (where the level of smoothing can be set) we detected peaks by the second derivative method.

Returning to Table 1, which shows some differences in the position of the spectral bands in our case and in Fine's paper, we must say that finding the correct positions of the spectral bands was, and still is, a problem, especially for the shoulder bands. We don't know what methods was used by Fine to determine these positions, but if the local maxima method can be used for bands with clear local maxima, it is not suitable for hidden peaks (shoulders) and therefore, in such cases, the results may be moderately incorrect.

We do not attempt to compare the data obtained with different techniques and methods, for finding the best (closest to real) peak positions of the absorption bands, but we shall merely remark that the results are dependent on the used method. A doubt can be raised (also considering the data of another reference [8]), concerning the accuracy of some earlier published data, especially for 661 and 691 nm peaks of $[\text{CoCl}_4]^{2-}$ Co-complex.

3. Conclusions

The absorption spectra of the CoCl_2 /acetone systems with addition of LiCl for stepwise formation of tetrahedral or pseudo-tetrahedral Co-complexes have been analyzed. The spectra of the tetrahedral-like, dichloro-, C_{2v} , $[\text{Co}^{2+}2\text{Cl}2\text{Ac}]$, trichloro-, C_{3v} , $[\text{Co}^{2+}3\text{Cl}1\text{Ac}]$ and real tetrahedral, tetrachloro-, T_d , $[\text{Co}^{2+}4\text{Cl}]^{2-}$, Co-complexes were detected and analyzed by the second derivative method. In addition, a computer simulated experiment, performed to study the method's performances, shows both its advantages and limitations. A doubt is raised concerning the accuracy in positioning the components of the absorption bands of the mentioned complexes given in some of the published data.

References

- [1] L.I. Katzin, E. Gebert, J. Amer. Chem. Soc. **75**, 2830 (1953).
- [2] D. Fine, J. Amer. Chem. Soc. **84**, 1139 (1962).
- [3] Ath. Trutia, M. Musa, Rev. Roum. Chim. **11**, 927 (1966).
- [4] M.S. Mendolia, G.C. Farrington, Electrochim. Acta **37**, 1695 (1992).
- [5] J. McBreen, X.Q. Yang, H.S. Lee, Y. Okamoto, Electrochim. Acta **40**, 2115 (1995).
- [6] G. Stanescu, Ath. Trutia, Proc. SPIE **5581**, 728 (2004).
- [7] A.B.Lever, Inorganic Electronic Spectroscopy, Elsevier (1968).
- [8] C. K. Jorgensen, Advances in Chemical Physics, vol. V, p. 98, Interscience Publ. (1963).